American Mineralogist, Volume 84, pages 596–606, 1999

Ca-Sr distribution among amphibole, clinopyroxene, and chloride-bearing solutions

J. NAJORKA,[1] M. GOTTSCHALK,[1,*] G. FRANZ,[2] AND W. HEINRICH[1]

[1]GeoForschungsZentrum Potsdam, Telegrafenberg A17, Potsdam 14473, Germany
[2]FG Petrologie, Technische Universität Berlin, Strasse des 17. Juni 135, Berlin 10623, Germany

ABSTRACT

The distribution of Sr between a 1 *M* $(Ca,Sr)Cl_2$ solution, (Ca,Sr)-tremolite and (Ca,Sr)-diopside was determined at 750 °C and 200 MPa. The synthesized crystals of (Ca,Sr)-tremolite (2000 × 30 μm) and (Ca,Sr)-diopside (1500 × 20 μm) were large enough for accurate electron microprobe analysis. The experimental results indicate that Ca^{2+} can be replaced completely by Sr^{2+} on the M4-site in tremolite and on the M2-site in diopside. The compositions of the product fluid were analyzed by atomic absorption spectroscopy. In both the (Ca,Sr)-tremolite-fluid and (Ca,Sr)-diopside-fluid systems, Sr strongly fractionated into the fluid. For bulk compositions having low Sr concentrations, mineral/fluid partition coefficients, $D_{Sr}^{mineral/fluid}$, of 0.045 for (Ca,Sr)-tremolite/fluid and 0.082 for (Ca,Sr)-diopside/fluid were derived. The experimental results were evaluated thermodynamically assuming Henry's law and simple mixing properties for $SrCl_2$ and $CaCl_2$ in the fluid. The mixing energies of the solids were calculated using a regular solution model. In the (Ca,Sr)-tremolite–$(Ca,Sr)Cl_2$ system, $\Delta\mu°$ is 59.0 kJ and W_{CaSr}^{amph} = 9.8 kJ. In the system (Ca,Sr)-diopside–$(Ca,Sr)Cl_2$ $\Delta\mu°$ is 30.8 kJ and W_{CaSr}^{px} is 11.7 kJ. The high $\Delta\mu°$ values and, to a much lesser extent, the W_{CaSr} values cause the strong fractionation of Sr into the fluid. The moderate values for W_{CaSr}^{amph} and W_{CaSr}^{px} strongly suggest that complete solid solution exists for (Ca,Sr)-tremolite and (Ca,Sr)-diopside at experimental run conditions. However, for the (Ca,Sr)-tremolite and (Ca,Sr)-diopside joins, limited miscibilities were calculated below 316 and 430 °C, respectively.

The experimentally derived thermodynamic properties were used to determine Ca/Sr ratios of Sr-rich metasomatic fluids that penetrated a metaeclogite in Bjørkedalen, southwest Norway. The derived Ca/Sr ratios from amphibole-fluid equilibria are in good agreement with those calculated from plagioclase-fluid equilibria.

INTRODUCTION

In most rock-forming minerals, Sr occurs as a minor or trace element and is preferentially incorporated in Ca-bearing phases. Because both Sr and Ca belong to the alkaline earth group of elements, they have a similar chemical behavior. The ionic radius in eightfold coordination is 1.12 Å for Ca^{2+} and 1.26 Å for Sr^{2+} (Shannon 1976).

Strontium enrichment in rocks is commonly induced by fluid-rock interactions (Grapes and Watanabe 1984; Theye and Seidel 1988). An example of extreme Sr metasomatism has been reported in a metaeclogite from Bjørkedalen, southwest Norway, by Brastad (1985) in which whole-rock SrO concentrations ranged up to 2.4 wt%. It is clear that information about trace element distribution between fluids and minerals is required for the reconstruction of such metasomatic processes.

Experimentally determined partition coefficients for Sr as a trace element between fluids and minerals have been reported for apatite (Ayers and Watson 1993), olivine (Brenan and Watson 1991), garnet (Brenan et al. 1995), clinopyroxene (Brenan et al. 1995; Adam et al. 1997; Ayers et al. 1997), and amphibole (Brenan et al. 1995; Adam et al. 1997). The distribution of Sr as a major element between fluids and minerals has been determined experimentally for (K,Sr)-feldspars by Kotelnikov and Chernysheva (1995), and Kroll et al. (1995) and for (Ca,Sr)-plagioclase by Kotelnikov and Chernysheva (1995), Kotelnikov et al. (1989), and Lagache and Dujon (1987). Thermodynamically relevant distribution coefficients and mixing models are not available for Sr-bearing amphiboles and pyroxenes. Although Sr-rich amphiboles and pyroxenes are only observed rarely in nature, both structures are flexible enough to incorporate significant Sr. Della Ventura and Robert (1990) and Robert et al. (1993) synthesized (K,Sr)-richterites with Sr^{2+} completely replacing Ca^{2+} on the M4-site. Benna (1982) and Benna et al. (1987) synthesized Sr-rich pyroxenes with at least 30 mol% of the Sr-diopside component.

Besides the geochemical interest in the quantification of Sr substitution in amphiboles and pyroxenes and the corresponding fluids/melts, there are questions of mineralogical importance. First, how much Ca^{2+} can be replaced by Sr^{2+} in the tremolite and diopside structure? Second, how can this substitution be described structurally and thermodynamically? An appropriate mixing model along the whole composition range provides the activity coefficients at low Sr concentrations (Henry's law constants), which are required for the geochemical applications.

The aim of this study is to determine the mixing behavior of Ca and Sr in amphibole and in pyroxene by considering the

*E-mail: gottschalk@gfz-potsdam.de

Ca_1Sr_{-1} exchange vector in the simplified (Ca,Sr)-tremolite [$(Ca,Sr)_2Mg_5Si_8O_{22}(OH)_2$] and (Ca,Sr)-diopside [$(Ca,Sr)MgSi_2O_6$] systems. This is accomplished by investigating experimentally the following exchange reactions:

$$\underset{Ca_2Mg_5Si_8O_{22}(OH)_2}{1\ \text{tremolite}} + 2\ [SrCl_2]^{aq} \leftrightarrow \underset{Sr_2Mg_5Si_8O_{22}(OH)_2}{1\ \text{Sr-tremolite}} + 2[CaCl_2]^{aq} \quad (1)$$

$$\underset{CaMgSi_2O_6}{1\ \text{diopside}} + 1\ [SrCl_2]^{aq} \leftrightarrow \underset{SrMgSi_2O_6}{1\ \text{Sr-diopside}} + 1\ [CaCl_2]^{aq} \quad (2)$$

The experimentally derived Ca-Sr equilibrium distribution coefficients among tremolite, diopside, and fluid allows the determination of the degree of fractionation of Sr into the fluid and the development of mixing models for the (Ca,Sr)-tremolite and the (Ca,Sr)-diopside solid solution series.

Experimental and analytical techniques

The experimental and analytical techniques are given in detail in Gottschalk et al. (1998) and are summarized briefly as follows. Standard cold-seal hydrothermal techniques were used. Temperatures were recorded using Ni-CrNi thermocouples, which were placed inside the autoclaves adjacent to the sample capsules. Total temperature and pressure uncertainties are estimated to be less than ±5 °C and ±10 MPa, respectively. The experiments were quenched by cooling the autoclaves with compressed air to <300 °C in about 3 min. All experiments were run for 21 days at 750 °C and 200 MPa. The chosen run duration was long enough to guarantee complete reaction.

Starting materials consisted of SiO_2, MgO, $Ca(OH)_2$, $Sr(OH)_2 \cdot 8H_2O$, and a 1 molar $CaCl_2$-$SrCl_2$ solution. The compositions of the starting mixtures are listed in Table 1. The $Sr(OH)_2 \cdot 8H_2O$ powder contained impurities of 2 wt% $SrCO_3$, 0.1 wt% Ba, and 0.05 wt% Ca. All other chemicals were of super pure quality. Stoichiometric oxide and hydroxide mixtures of 15–25 mg having bulk compositions on the tremolite–Sr-tremolite join, with 5 wt% of SiO_2 in excess to compensate for SiO_2 solubility at experimental conditions, were used along with 50–200 μL of a one molar (Ca,Sr)Cl_2-solution. Run 8 and 14 had bulk compositions on the diopside–Sr-diopside join. Two different $(Ca+Sr)^{solid}/(Ca+Sr)^{total}$ ratios of 0.42–0.49 (runs 1 to 15) and 0.16–0.18 (runs 16 to 23) were used. All experiments were performed in 25 and 35 mm long gold capsules with inner diameters of 2.6 and 4.6 mm, respectively, and wall thicknesses of 0.2 mm.

After the runs were completed, the unopened capsules were cleaned with a dilute HCl solution and hot distilled water. The gold tubes were then cut open in distilled water. The run products were washed out with double-distilled water and then filtered. All product fluid was collected and diluted to yield a total of 100 mL solution.

The solid products were examined by optical microscopy, scanning electron microscopy (SEM), high-resolution transmission electron microscopy (HRTEM), electron microprobe (EMP), powder X-ray diffraction (XRD) with Rietveld analysis, and fourier transform infrared spectroscopy (IR). The fluids were analyzed for Ca, Sr, and Mg by atomic absorption spectroscopy (AAS).

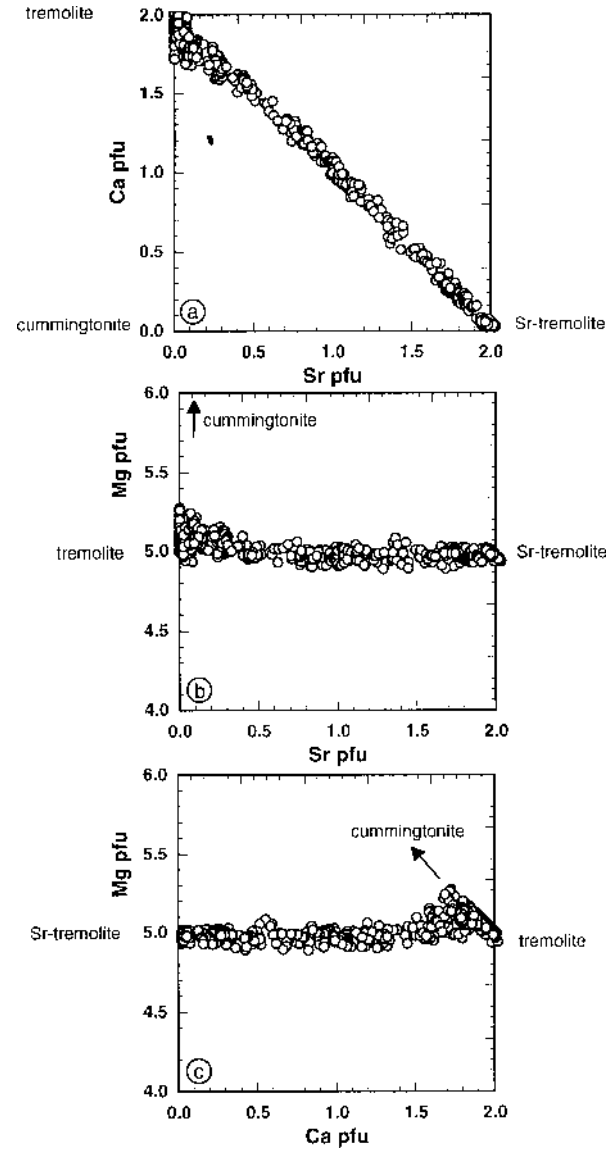

Figure 1. Formula proportions of Mg, Ca, and Sr in (Ca,Sr)-tremolite from EMP point analyses. **(a)** Ca vs. Sr content. **(b)** Mg vs. Sr content. **(c)** Mg vs. Ca content. Values >5 for Mg correspond to Mg^{2+} on the M4-site (cummingtonite). Mg is variable in Ca-rich tremolites with maximum cummingtonite contents of 15 mol%.

Results

The reaction products of runs on the (Ca,Sr)-tremolite join consisted of 29–100 wt% tremolite, 0–60 wt% diopside, 0–10 wt% enstatite, and 0–13 wt% quartz. In the reaction products from runs 18, 20, and 21, up to 11 wt% forsterite was found instead of quartz. Talc (2 wt%) was found only in run 17. The products from runs 8 and 14 on the (Ca,Sr)-diopside join consisted of 95 wt% diopside and 5 wt% quartz.

Results from the structural characterization of the synthesized (Ca,Sr)-tremolites and (Ca,Sr)-diopsides by XRD, SEM, HRTEM, and IR are discussed in detail by Gottschalk et al. (1998). Summarizing, the crystals of (Ca,Sr)-tremolite were up to 2000 μm long and 30 μm wide whereas those of (Ca,Sr)-

TABLE 1. Compositions of starting mixtures and run product fluids

Run	1	2	5	6	8	9	10	11	12	13	14	15
Solid starting materials (mg)												
SiO_2	10.90	11.25	10.82	10.35	7.16	11.50	11.37	11.62	11.75	10.96	7.87	11.25
MgO	4.36	4.50	4.32	4.27	2.29	4.59	4.54	4.64	4.70	4.38	2.52	4.50
$Ca(OH)_2$	0.00	0.99	2.85	2.51	0.00	1.69	1.34	2.05	2.41	0.16	1.54	0.99
$Sr(OH)_2 \cdot 8\ H_2O$	11.48	8.30	1.14	2.25	15.09	6.05	7.19	4.90	3.71	10.96	8.29	8.30
Fluid starting materials												
Fluid (µL)	60	50	50	50	60	60	60	60	60	60	60	60
Sr/(Sr+Ca)	1.000	0.840	0.100	0.200	1.000	0.500	0.600	0.400	0.300	0.950	0.500	0.700
Molarity	1.0	1.0	1.0	1.0	1.0	1.0	1.0	1.0	1.0	1.0	1.0	1.0
ρ fluid (g/ccm)	1.134	1.126	1.090	1.095	1.134	1.110	1.115	1.105	1.100	1.132	1.110	1.120
Fluid (mg)	68.05	56.32	54.52	54.76	68.05	66.59	66.88	66.30	66.00	67.91	66.59	67.18
Total run charge (mmol)												
Si	0.181	0.187	0.180	0.172	0.119	0.191	0.189	0.193	0.196	0.182	0.131	0.187
Mg	0.108	0.112	0.107	0.106	0.057	0.114	0.113	0.115	0.117	0.109	0.063	0.112
Ca	0.000	0.021	0.084	0.074	0.000	0.053	0.042	0.064	0.075	0.005	0.051	0.031
Sr	0.103	0.073	0.009	0.018	0.117	0.053	0.063	0.042	0.032	0.098	0.061	0.073
H_2O total	3.638	3.002	2.782	2.816	3.760	3.475	3.509	3.441	3.405	3.623	3.549	3.543
H_2O in tremolite	0.022	0.022	0.021	0.021	–	0.023	0.023	0.023	0.023	0.022	-	0.022
H_2O in fluid	3.616	2.980	2.761	2.795	3.760	3.452	3.486	3.418	3.382	3.601	3.549	3.521
Theoretical molarity	0.911	0.920	0.982	0.972	0.881	0.947	0.940	0.956	0.964	0.915	0.925	0.932
Final fluid composition												
Mg^{2+} (mmol)	<0.001	0.001	0.003	0.002	<0.001	0.002	<0.001	<0.001	0.002	0.001	<0.001	0.001
Ca^{2+} (mmol)	<0.001	0.002	0.032	0.030	<0.001	0.005	0.003	0.012	0.026	<0.001	0.005	0.004
Sr^{2+} (mmol)	0.047	0.043	0.010	0.017	0.048	0.019	0.024	0.024	0.029	0.052	0.032	0.051
Estimated molarity	0.739	0.825	0.833	0.914	0.721	0.398	0.450	0.602	0.890	0.805	0.580	0.847

Notes: r fluid derived by interpolation from the densities of 1 *M* $CaCl_2$ solution (1.086 g/ccm) and 1*M* $SrCl_2$ solution (1.134 g/ccm). H_2O in tremolite is the maximum content of water in solids in the case of only tremolite and no diopside formation. The theoretical molarity is the value at the end of the run considering H_2O formation from hydroxides and H_2O consumption from the formation of tremolite.

TABLE 2. Average compositions of tremolite–Sr-tremolite solid solutions determined by EMP

Run	1	2a	2b	5	6	9	10	11	12	13	15	16
Amphibole composition (wt%)												
No. of analysis	87	65	12	34	26	21	11	12	29	47	28	22
SiO_2	52.83	56.31	54.63	59.38	59.35	58.89	57.52	58.64	59.40	53.19	57.95	58.80
MgO	21.59	22.92	21.97	25.05	24.97	24.47	23.66	24.39	24.75	21.76	23.73	24.67
CaO	0.27	7.58	3.42	12.99	13.17	12.80	11.40	12.92	13.26	1.48	10.40	11.19
SrO	23.02	10.36	17.22	0.18	0.22	1.22	3.50	0.68	0.33	21.00	5.48	3.39
Σ	97.71	97.17	97.24	97.60	97.71	97.38	96.08	96.64	97.74	97.43	97.57	98.05
Standard deviation (2σ)												
ΔSiO_2	1.41	2.31	2.47	1.43	1.57	1.24	1.06	1.54	1.47	1.61	1.73	1.56
ΔMgO	0.42	0.85	0.95	1.02	0.68	0.91	0.62	0.83	0.82	0.97	0.73	1.08
ΔCaO	0.18	2.10	1.40	0.92	0.56	0.47	0.47	0.58	0.42	0.69	0.64	0.43
ΔSrO	0.83	3.79	2.42	0.22	0.36	0.14	0.84	0.39	0.49	1.58	0.99	1.18
Amphibole composition on the basis of 8 Si atoms												
Sr	1.98	0.87	1.47	0.00	0.01	0.07	0.27	0.03	0.02	1.79	0.45	0.27
Ca	0.04	1.16	0.54	1.90	1.92	1.89	1.72	1.92	1.94	0.23	1.56	1.65
Mg	4.98	4.97	4.99	5.10	5.07	5.04	5.00	5.05	5.04	4.98	4.99	5.08
Si	8.00	8.00	8.00	8.00	8.00	8.00	8.00	8.00	8.00	8.00	8.00	8.00

diopside were up to 150 µm long and 20 µm wide. The tremolite crystals from Ca-rich bulk compositions were more fibrous than those from Sr-rich bulk compositions. Tremolite and diopside crystals from most runs were well ordered with very low concentrations of chain multiplicity faults. The concentration of chain multiplicity faults increased somewhat with increasing Ca-content of the (Ca,Sr)-tremolites but exceeded 5% rarely.

Crystals of (Ca,Sr)-tremolite and (Ca,Sr)-diopside were large enough for accurate EMP analysis. The run products were mounted in epoxy and polished. Between 4 and 87 analyses were obtained on the amphiboles produced in each run. Formula proportions of Ca, Sr, and Mg of from single-point EMP analyses (Ca,Sr)-tremolite are plotted in Figure 1. These analyses cover the entire compositional range between the tremolite and Sr-tremolite end-members and reveal a continuous (Ca,Sr)-tremolite solid solution series. There is, however, a small but significant deviation from the ideal Ca_1Sr_{-1} substitution, indicating the presence of some cummingtonite [$Mg_2Mg_5Si_8O_{22}(OH)_2$] component. This deviation was below ±0.05 pfu for most single point analyses of the (Ca,Sr)-tremolites except for very Ca-rich compositions in which the deviations were as high as ±0.15 pfu. For these Ca-rich tremolites, the Ca content has a negative correlation with the Mg content (Fig. 1c), which reflects the variable amount of the cummingtonite component [$X_{cum} = Mg^{M4}/(Ca+Sr+Mg)^{M4}$]. All amphiboles, therefore, are solid solutions among tremolite, Sr-tremolite, and cummingtonite end-members.

The average composition of the amphiboles is given in Table 2 and Figure 2. For amphiboles with $X_{Sr\text{-}tr}<0.15$ [$X_{Sr\text{-}tr} = Sr^{M4}/(Ca+Sr+Mg)^{M4}$], the observed average cummingtonite content was below 0.07. For amphiboles with higher $X_{Sr\text{-}tr}$-contents, X_{cum} was below 0.01. Most of the synthesized amphiboles were homogeneous within ±0.03 $X_{Sr\text{-}tr}$ (2σ), except for (Ca-Sr)-tremolites from runs 2, 13, 20, and 23. Tremolite compositions from runs 13 and 20 showed variations of ±0.06 and those from runs

TABLE 1—*Extended*

16	17	18	20	21	22	23
11.14	11.38	11.25	9.92	10.10	10.17	9.87
4.45	4.54	4.49	3.96	4.03	4.06	3.94
0.65	1.34	0.99	0.29	0.79	1.00	0.14
9.38	7.19	8.29	9.41	7.80	7.13	9.88
200	200	200	200	200	200	200
0.800	0.600	0.700	0.900	0.735	0.670	0.950
1.0	1.0	1.0	1.0	1.0	1.0	1.0
1.124	1.115	1.120	1.129	1.121	1.118	1.132
224.89	222.94	223.92	225.87	224.26	223.63	226.35
0.185	0.189	0.187	0.165	0.168	0.169	0.164
0.110	0.113	0.112	0.098	0.100	0.101	0.098
0.049	0.098	0.073	0.024	0.064	0.079	0.012
0.195	0.147	0.171	0.215	0.176	0.161	0.227
11.156	11.088	11.122	11.153	11.103	11.083	11.168
0.022	0.023	0.022	0.020	0.020	0.020	0.020
11.134	11.065	11.100	11.133	11.083	11.063	11.148
0.976	0.981	0.979	0.976	0.980	0.981	0.975
0.001	0.005	0.001	<0.001	<0.002	0.004	<0.001
0.016	0.054	0.016	0.006	0.026	0.041	0.003
0.161	0.132	0.100	0.171	0.143	0.144	0.160
0.875	0.916	0.597	0.874	0.844	0.910	0.814

TABLE 2—*Extended*

17	18	20	21	22	23a	23b
8	18	4	13	2	6	16
59.25	59.04	55.43	59.42	56.78	55.50	53.74
24.65	24.49	22.99	25.23	23.83	22.86	22.06
12.31	11.88	8.18	12.07	12.20	5.25	2.84
0.61	1.62	8.94	1.01	0.81	14.09	18.54
96.82	97.04	95.53	97.74	93.62	97.70	97.17
1.29	2.50	2.16	1.54	2.68	1.54	1.60
1.12	1.60	0.68	0.80	0.59	0.75	0.57
0.49	0.80	0.78	0.54	0.09	0.83	1.19
0.54	0.52	1.59	0.52	0.40	1.52	2.15
0.04	0.13	0.77	0.10	0.09	1.19	1.59
1.84	1.77	1.25	1.76	1.86	0.80	0.44
5.12	5.10	4.98	5.13	5.05	5.00	4.96
8.00	8.00	8.00	8.00	8.00	8.00	8.00

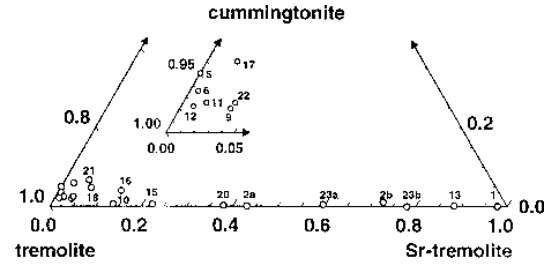

FIGURE 2. Average compositions of (Ca,Sr)-tremolites from all runs plotted on a tremolite–Sr-tremolite–cummingtonite ternary diagram. Ca-rich (Ca,Sr)-tremolites show variable contents of the cummingtonite component. For runs 2 and 23, the compositions of both (Ca,Sr)-tremoite populations having different values of $X_{Sr\text{-}tr}$ are denoted as 2a,b and 23a,b, respectively.

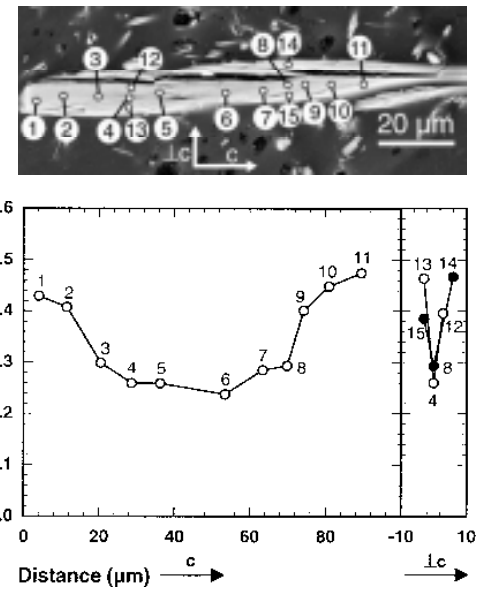

FIGURE 3. Ca-Sr zonation in a tremolite crystal from run 2 along and perpendicular the crystallographic c direction. The Sr concentration increases toward the rim. Numbers denote individual analysis spots.

2 and 23 of ±0.16 and ±0.11, respectively (all 2σ). In runs 2 and 23, two different compositional types of (Ca,Sr)-tremolite were distinguished by EMP, XRD, and IR-spectroscopy with average $X_{Sr\text{-}tr}$ of 0.44 and 0.73 for run 2 and 0.59 and 0.79 for run 23 (see also Gottschalk et al. 1998). Besides the two compositional types, large (Ca,Sr)-tremolite crystals from run 2 show a clear zonation (Fig. 3). Cores from such grains have $X_{Sr\text{-}tr}$ = 0.25 and rims have $X_{Sr\text{-}tr}$ = 0.43–0.46. Such zonations were never observed in any (Ca,Sr)-tremolite crystals from other runs.

The diopsides were solid solutions of diopside and Sr-diopside end-members with only small amounts of the enstatite component. Variations in the amount of the enstatite content were somewhat larger for Ca-rich diopsides than for Sr-rich diopsides (Figs. 4a and 4b). The average compositions of the diopsides from each run are listed in Table 3. The average amount of the enstatite component (X_{en}) did not exceed 0.05 and was below 0.02 in most runs. Variations in $X_{Sr\text{-}di}$ in the pyroxenes for each run was below ±0.03 (2σ) except for (Ca,Sr)-diopsides from runs 1, 2, 13, 14, and 15 in which the variations in $X_{Sr\text{-}di}$ were <0.06. As for the tremolites from run 2, the pyroxenes also show a rather large compositional variation of ±0.13 in $X_{Sr\text{-}di}$. No diopsides formed in runs 20 and 23.

The Ca^{2+}, Sr^{2+}, and Mg^{2+} concentrations of the final fluid are listed in Table 1. The error (2σ) was estimated to be <3% relative. The concentration of Cl^- was not measured. The molarity was estimated from Ca^{2+}, Sr^{2+} and Mg^{2+} concentrations assuming that these were the only cations present in the fluid. Concentrations of Mg^{2+} were always very low and Mg/(Ca+Sr+Mg) values (cation fraction, here of Mg) exceeded 0.02 only for runs with Ca-rich bulk compositions. It is interesting to note that for Ca-rich tremolites with a highly variable cummingtonite content (Fig. 2), the variation of Mg in the fluid was also high (Fig. 5). The estimated molarity (0.40–0.92) was always lower than the theoretical molarity (0.88–0.98), which

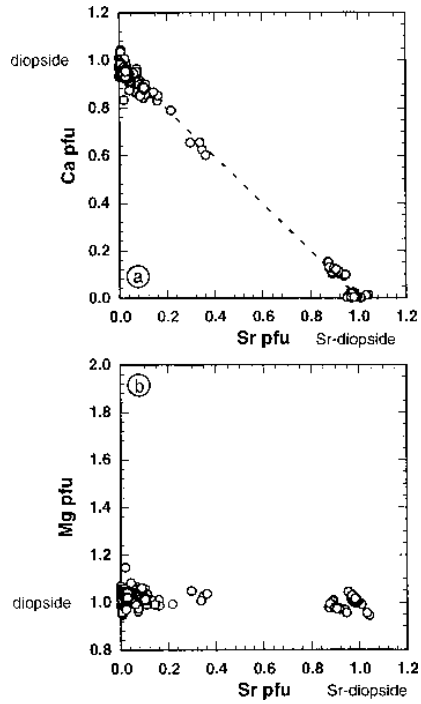

FIGURE 4. Formula proportions of Mg, Ca, and Sr in (Ca,Sr)-diopside from EMP point analyses. (**a**) Ca vs. Sr content. (**b**) Mg vs. Sr content. Values >1 of Mg correspond to incorporation of Mg^{2+} on the M2-site (enstatite component).

can be calculated from the run charges under the assumption of complete reaction (Table 1).

Figures 6 and 7 show reciprocal ternary plots for the systems (Ca,Sr)-tremolite–$(Ca,Sr)Cl_2$ and (Ca,Sr)-diopside–$(Ca,Sr)Cl_2$, respectively, along with the compositions of coexisting solids and fluids from Table 4. Figure 8 illustrates the distribution of Sr between (Ca,Sr)-tremolite and fluid, (Ca,Sr)-diopside and fluid, and (Ca,Sr)-tremolite and (Ca,Sr)-diopside. The essential point is that in both systems (tremolite/fluid and diopside/fluid) Sr fractionates preferentially into the fluid.

INTERPRETATION AND DISCUSSION

(Ca,Sr)-tremolites from most runs were homogeneous (± 0.03 $X_{Sr\text{-}tr}$). Only in runs 2 and 23 were two populations of (Ca,Sr)-tremolites with different compositions identified by EMP and XRD (see also Gottschalk et al. 1998); these have $X_{Sr\text{-}tr}$ = 0.44 and 0.73 in run 2, and 0.59 and 0.79 in run 23 (labeled as 2a, 2b, 23a, and 23b in Table 2). The two populations from either run cannot be interpreted as coexisting (Ca,Sr)-tremolites at a miscibility gap but rather as a result of a complex reaction path during those runs. It is possible that at the very beginning of those two experiments, fluctuations in the composition of the fluid occurred due to inhomogeneities of the starting materials within each capsule. The fluid composition also may have depended on the different dissolution rates of the starting materials. Such local compositional variations in the fluid initially may have produced (Ca,Sr)-tremolites that were not in equilibrium with the bulk fluid but were metastable. The sensitivity of the tremolite composition to compositional variations of the fluid is enhanced for fluid compositions with Sr/(Ca+Sr) > 0.95 in comparison to fluids with lower Sr contents (Fig. 8). It is obvious from Figure 8a that in this range, the distribution of Sr between (Ca,Sr)-tremolite and fluid is very flat. Small compositional variations in the fluid lead to amplified variations in the coexisting solids. The final fluids of runs 2 and 23 had compositions of Sr/(Ca+Sr) = 0.954 and 0.981. The amphiboles in runs 2 and 23, which do have X_{Sr} closest to their respective bulk compositions, are the most probable candidates for being in equilibrium with the fluid (amphibole 2a and 23b from Table 2). This approach to equilibrium is also supported by the observation that these amphiboles yield thermodynamically consistent, subparallel tie-lines.

Figure 3 shows that in run 2, besides the two distinct tremolite populations, large (Ca,Sr)-tremolite crystals were zoned with cores enriched in Ca relative to the rims. It is reasonable to assume that the (Ca,Sr)-tremolite compositions of the rims were in equilibrium with the final fluid. The average composition of most small crystals from run 2 (65 EMP analyses; $X_{Sr\text{-}tr}$ = 0.44) were practically identical to the rim composition (0.43–0.46) of the grain shown in Figure 3. Such a zonation is interpreted as the result of a fractional crystallization process (for

TABLE 3. Average compositions of diopside–Sr-diopside solid solutions as determined by EMP

Run	1	2	5	6	8	9	10	11	12	13	14	15
Pyroxene composition (wt%)												
No. of analysis	14	5	7	7	37	28	6	2	12	12	9	13
SiO_2	44.81	52.07	55.83	55.77	45.14	55.79	54.54	54.86	55.65	46.22	54.67	54.91
MgO	14.77	17.21	18.05	19.00	14.95	18.61	18.10	18.09	19.00	15.34	18.30	18.21
CaO	0.41	15.91	25.17	24.75	0.05	24.52	22.41	24.34	25.35	2.59	23.25	22.38
SrO	40.07	13.79	0.22	0.26	39.84	1.22	4.29	1.15	0.46	36.15	3.54	5.14
Σ	100.06	98.97	99.28	99.78	99.98	100.14	99.35	98.44	100.45	100.31	99.75	100.64
Standard deviation (2σ)												
ΔSiO_2	1.11	2.89	1.17	1.30	0.92	1.45	1.20	0.54	0.97	1.04	1.25	0.91
ΔMgO	0.96	0.50	1.20	0.68	0.47	1.42	0.50	1.75	0.65	0.61	0.47	1.09
ΔCaO	0.14	4.58	0.87	1.84	0.03	1.66	0.92	1.03	0.94	0.83	1.61	2.50
ΔSrO	1.52	5.38	0.3	0.34	1.8	1.45	0.94	0.44	0.66	1.06	2.63	2.81
Pyroxene composition on the basis of 2 Si atoms												
Sr	0.99	0.31	0.00	0.00	0.99	0.02	0.09	0.02	0.01	0.90	0.07	0.11
Ca	0.02	0.67	1.00	0.97	0.00	0.96	0.90	0.97	0.98	0.12	0.92	0.89
Mg	0.99	1.02	1.00	1.03	1.01	1.02	1.01	1.01	1.02	0.98	1.01	1.00
Si	2.00	2.00	2.00	2.00	2.00	2.00	2.00	2.00	2.00	2.00	2.00	2.00

detailed discussion see Zimmermann et al. 1997a). At the beginning of the run, X_{Sr} of the fluid should be close to that of the bulk composition, which is always lower in Sr than the final fluid. Because Sr fractionates strongly into the fluid, (Ca,Sr)-tremolites crystallizing initially were more Ca-rich than those in equilibrium at the end of the experiment. This process is especially enhanced for Sr-rich bulk compositions and resulting final fluids with a X_{Sr} of >0.95 (see discussion above). This is supported by observations made from run 20, which was performed at conditions almost identical to run 2, except for the fluid/solid ratio. In run 20, there was four times as much fluid as amphibole compared with run 2, and therefore the fluid had a much higher buffer capacity. Significantly smaller variations in composition were observed in amphiboles from run 20 compared with run 2. Chemical variations in (Ca,Sr)-tremolites from run 2 ($\Delta X_{Sr\text{-}tr} = \pm 0.16\ 2\sigma$) were, by far, the greatest ones observed.

We emphasize, however, that in the vast majority of the runs, the (Ca,Sr)-tremolites and (Ca,Sr)-diopsides were homogeneous with a compositional variation (2σ) in $X_{Sr\text{-}tr}$ of less than ± 0.03 and in $X_{Sr\text{-}di}$ of less than ± 0.05 (Figs. 6, 7, and 8).

No (Ca,Sr)-diopside compositions were observed in the range between $0.31 > X_{Sr\text{-}di} > 0.90$. In principle, this might be due either to a limited miscibility or to an extreme fractionation behavior. As shown above, Sr fractionation for pyroxene/fluid is even more enhanced than for the amphibole/fluid system. Pyroxenes with a $X_{Sr\text{-}di} = 0.31$ coexist with a fluid having $X_{Sr} = 0.954$ whereas pyroxenes with $X_{Sr\text{-}di} = 0.90$ coexist with a fluid having $X_{Sr} = 0.975$. Thus, a difference in X_{Sr} in the fluid of only 0.021 leads to a change in $X_{Sr\text{-}di}$ from 0.31 to 0.90 in the pyroxenes. If this effect is disregarded, one might argue that a fluid composition anywhere between these values would coexist with two diopside compositions. However, the thermodynamic treatment of the system (see below) reveals that a miscibility gap along the (Ca,Sr)-diopside join at the experimental conditions is highly improbable. The absence of compositions in the range of $0.31 < X_{Sr\text{-}di} < 0.90$ is simply the result of the chosen bulk compositions.

The molarity in the fluid calculated from the experimentally determined cation concentrations was always somewhat lower than the theoretical values calculated from the starting materials (Table 1). This is most likely due to fluid loss when opening the capsules and probably also to insufficient washing of the solid run products. However the important cation ratios are not affected by fluid loss.

TABLE 3—*Extended*

16	17	18	21	22
15	18	16	8	16
54.94	55.67	55.18	55.67	53.26
18.95	19.45	19.11	19.13	18.71
22.26	24.34	23.36	23.75	24.10
4.69	0.87	2.24	1.56	0.89
100.84	100.34	99.88	100.11	96.96
1.29	1.87	1.54	1.40	1.47
0.72	0.41	1.06	0.64	0.73
0.97	0.95	0.94	1.66	1.07
0.8	0.66	0.53	0.34	0.41
0.10	0.02	0.05	0.04	0.03
0.87	0.94	0.91	0.92	0.95
1.03	1.04	1.04	1.04	1.03
2.00	2.00	2.00	2.00	2.00

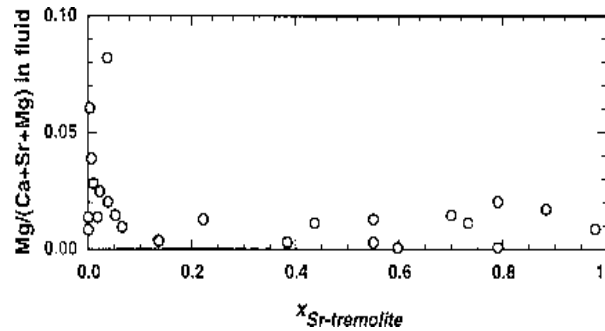

FIGURE 5. Mg concentration in the product fluid vs. Sr-concentrations in (Ca,Sr)-tremolite. Higher Mg variations in the fluid correspond with increased cummingtonite contents in Ca-rich (Ca,Sr)-tremolites and -diopsides (see Figs. 2 and 4).

The reciprocal ternary plots of the systems (Ca,Sr)-tremolite–$(Ca,Sr)Cl_2$ and (Ca,Sr)-diopside–$(Ca,Sr)Cl_2$ (Figs. 6 and 7) show subparallel tie-lines. This is a good argument for thermodynamic equilibrium in the runs because such subparallel tie-lines are required for thermodynamic consistency. If only (Ca,Sr)-tremolite had formed, the tie-lines would coincide with the bulk compositions plotted in Figure 6. That in some cases the bulk compositions are slightly off the tie-lines is mainly due to the formation of (Ca,Sr)-diopside and cummingtonite component in the (Ca,Sr)-tremolites. The offset is most pronounced for the (Ca,Sr)-tremolites from runs 2 and 15. For all other runs, the tie-lines are very close to their bulk composition.

Zimmermann et al. (1997b) tried to demonstrate equilibrium of the Na-K-Ca exchange between amphibole and an aqueous chloride solution with reversed experiments. They showed that such experiments did not approach overall equilibrium corresponding to the respective bulk chemistry. Due to a dissolution fractional-crystallization process, only small amounts of the starting amphiboles were dissolved and the product amphibole precipitated around them as very thin epitaxial rims. Although it can be assumed that these rims were in equilibrium with the fluid present at the time of precipitation, the fluid did evolve with time together with the coexisting amphibole rims. As a result a large array of amphibole compositions was observed that made the runs useless for the demonstration of equilibrium. Synthesizing amphiboles with an excess of fluid, however, allows the exchange of cations between fluid and solid to a much larger extent (Zimmermann et al. 1997a), which minimizes the effect of fractional crystallization.

Summarizing, we believe that equilibrium distributions were achieved based on three main arguments. First, in the vast majority of the runs, the (Ca,Sr)-tremolites are within a very narrow compositional range. Second, the (Ca,Sr)-tremolites are well crystallized with almost no stacking or multiplicity faults (Gottschalk et al. 1997). Third, the phase relations in the reciprocal ternary show overall consistency. All these are good arguments for thermodynamic equilibrium.

TABLE 4. Ca, Sr, and Mg concentrations in terms of molar ratios in coexisting amphibole, pyroxene, and fluid

Run	1	2	5	6	8	9	10	11	12	13	14	15
					fluid							
$X_{SrC_2} \times 100$	1.288	1.417	0.340	0.589	1.255	0.541	0.687	0.699	0.855	1.411	0.880	1.423
$X_{CaCl_2} \times 100$	0.003	0.052	1.154	1.065	0.003	0.136	0.082	0.352	0.755	0.011	0.132	0.098
$X_{MgCl_2} \times 100$	0.011	0.017	0.096	0.067	0.011	0.060	0.003	0.014	0.047	0.025	0.014	0.020
X_{H_2O}	0.987	0.985	0.984	0.983	0.987	0.993	0.992	0.989	0.983	0.986	0.990	0.985
Sr/(Ca+Sr+Mg)	0.990	0.954	0.214	0.342	0.990	0.734	0.890	0.655	0.516	0.975	0.857	0.923
ΔSr/(Ca+Sr+Mg)(2σ)	0.001	0.003	0.015	0.020	0.001	0.014	0.008	0.019	0.021	0.001	0.010	0.005
Ca/(Ca+Sr+Mg)	0.002	0.035	0.725	0.619	0.002	0.184	0.106	0.331	0.456	0.008	0.129	0.064
Mg/(Ca+Sr+Mg)	0.008	0.011	0.061	0.039	0.008	0.082	0.004	0.014	0.028	0.017	0.014	0.013
					Amphibole							
$X_{Sr\text{-}tr}$	0.978	0.437	0.003	0.006	-	0.037	0.135	0.017	0.010	0.883	-	0.221
$\Delta X_{Sr\text{-}tr}$ (2σ)	0.025	0.158	0.002	0.002	-	0.006	0.022	0.004	0.005	0.061	-	0.034
X_{tr}	0.021	0.579	0.950	0.959	-	0.943	0.859	0.958	0.969	0.115	-	0.773
X_{cum}	0.001	0.001	0.047	0.035	-	0.020	0.006	0.025	0.021	0.002	-	0.006
Pyroxene												
$X_{Sr\text{-}di}$	0.982	0.312	0.001	0.003	0.980	0.020	0.089	0.015	0.008	0.900	0.069	0.111
$\Delta X_{Sr\text{-}di}$ (2σ)	0.046	0.130	0.005	0.005	0.029	0.020	0.018	0.010	0.003	0.048	0.056	0.063
X_{di}	0.019	0.665	0.998	0.965	0.018	0.960	0.899	0.965	0.975	0.119	0.921	0.887
X_{en}	0.007	0.023	0.001	0.032	0.018	0.020	0.012	0.020	0.017	0.001	0.010	0.012
$X_{Sr\text{-}bulk}$	1.000	0.774	0.100	0.200	1.000	0.500	0.600	0.400	0.300	0.950	0.546	0.700
$\Delta X_{Sr\text{-}bulk}$ (2σ)	0.000	0.015	0.008	0.014	0.000	0.021	0.020	0.020	0.018	0.004	0.021	0.018
(Sr+Ca) solid/bulk	0.419	0.472	0.461	0.459	0.486	0.431	0.429	0.435	0.437	0.420	0.464	0.427
					Reaction 1: tremolite + 2 $CaCl_2$ ↔ Sr-tremolite + 2 $SrCl_2$							
$\ln K_D$	-4.62	-7.18	-9.07	-8.96	-	-9.25	-7.95	-9.41	-9.50	-5.65	-	-7.84
$\Delta \ln K_D$	2.36	1.30	1.35	0.69	-	0.36	0.42	0.50	1.02	1.20	-	0.43
$D_{Sr}^{amph/fluid}$	3.28	1.41	0.04	0.05	-	0.31	0.90	0.11	0.05	2.75	-	0.74
					Reaction 2: diopside + $CaCl_2$ ↔ Sr-diopside + $SrCl_2$							
$\ln K_D$	-2.20	-4.07	-5.21	-5.25	-0.19	-5.14	-4.44	-4.65	-4.50	-2.84	-4.49	-4.75
$\Delta \ln K_D$	2.57	0.61	2.92	1.66	1.52	0.92	0.24	0.55	0.43	0.54	0.87	0.64
$D_{Sr}^{amph/fluid}$	7.41	2.57	0.08	0.06	7.59	0.51	1.55	0.33	0.11	6.36	0.97	0.97

Note: x_{SrCl2} = $SrCl_2$/($SrCl_2$+$CaCl_2$+$MgCl_2$+H_2O) mole fraction of $SrCl_2$ in the fluid, Sr/(Ca+Sr+Mg) molar cation fraction of Sr in the fluid, $X_{Sr\text{-}tr}$ = Sr/(Sr+Ca+Mg) mole fraction of Sr on M4 in tremolite, $X_{Sr\text{-}di}$ = Sr/(Sr+Ca+Mg) mole fraction of Sr on M2 in diopside, $X_{Sr\text{-}bulk}$ = Sr/(Sr+Ca) molar cation fraction of Sr in the bulk (equivalent definitions for $X_{Ca\text{-}fluid}$, $X_{Mg\text{-}fluid}$, X_{tr}, X_{cum}, X_{di}, and X_{en}). For the calculation of the K_D-values more digits were used than given in Table 4.

THERMODYNAMIC EVALUATION

The mixing parameters for the (Ca,Sr)-tremolite solid solutions have been extracted assuming thermodynamic equilibrium. At constant pressure and temperature, an equilibrium such as Equation 1 can be formulated thermodynamically with the expressions

$$\Delta\mu^\circ + RT\ln\frac{a_{Sr-tr}^{amph}(a_{CaCl_2}^{aq})^2}{a_{tr}^{amph}(a_{SrCl_2}^{aq})^2} = 0 \quad (3)$$

and

$$\Delta\mu^o = \mu_{Sr-tr}^o + 2\mu_{CaCl_2}^o - \mu_{tr}^o - 2\mu_{SrCl_2}^o \quad (4)$$

where a are the activities of the components and μ° are the standard state chemical potentials. Mixing in (Ca,Sr)-tremolites takes place on the two M4-sites. Because the M4-site has a multiplicity of two, the activities of tremolite and Sr-tremolite are written as the squared product of the M4-site occupancy and its activity coefficient:

$$a_{tr}^{amph} = \left(X_{Ca}^{amph}\gamma_{Ca}^{amph}\right)^2 \quad (5)$$

$$a_{Sr-tr}^{amph} = \left(X_{Sr}^{amph}\gamma_{Sr}^{amph}\right)^2 \quad (6)$$

Using the definitions for the activities of $CaCl_2$ and $SrCl_2$ ($a_i = x_i\,\gamma_i$) and the definition of the distribution coefficient K_D,

$$K_D = \frac{X_{Sr}^{amph}X_{CaCl_2}^{aq}}{X_{Ca}^{amph}X_{SrCl_2}^{aq}} \quad (7)$$

Equation 3 becomes:

$$\Delta\mu^o + 2RT\ln K_D + 2RT\ln\frac{\gamma_{Sr}^{amph}\gamma_{CaCl_2}^{aq}}{\gamma_{Ca}^{amph}\gamma_{SrCl_2}^{aq}} = 0 \quad (8)$$

Because the runs were conducted with a 1 molar solution, it is reasonable to assume that Henry's law is obeyed in the fluid. Furthermore, it is assumed that the Henry's constants of both $CaCl_2$ and $SrCl_2$ (or Ca^{2+} and Sr^{2+}) are equal because of their chemical similarities. This simplifies Equation 8 to:

$$\Delta\mu^o + 2RT\ln K_D + 2RT\ln\frac{\gamma_{Sr}^{amph}}{\gamma_{Ca}^{amph}} = 0 \quad (9)$$

If the Henry's constants of $CaCl_2$ and $SrCl_2$ (or Ca^{2+} and Sr^{2+}) are not equal, a constant value is simply added to $\Delta\mu^\circ$, but Equation 9 still holds.

Ideal mixing, i.e., $\gamma_i = 1$, on the M4-site in the amphiboles is improbable. The simplest activity model is that of a regular solution. Using the formulation of Wohl (1946), a regular solution in the ternary system tremolite–Sr-tremolite–cummingtonite, including a ternary interaction parameter, can be formulated as

$$G_{M4}^{EM} = X_{Ca}X_{Sr}W_{CaSr} + X_{Ca}X_{Mg}W_{CaMg} + X_{Sr}X_{Mg}W_{SrMg} + X_{Ca}X_{Sr}X_{Mg}C \quad (10)$$

where W_{CaSr}, W_{CaMg}, and W_{SrMg} are the binary interaction parameters and C is the ternary interaction parameter. The activity coefficient of a component can be derived by multiplying Equa-

16	17	18	20	21	22	23
1.427	1.176	0.895	1.508	1.273	1.275	1.415
0.141	0.475	0.139	0.055	0.235	0.363	0.027
0.005	0.042	0.010	0.004	0.022	0.034	0.001
0.984	0.983	0.990	0.984	0.985	0.983	0.986
0.908	0.694	0.858	0.962	0.832	0.763	0.981
0.007	0.017	0.010	0.003	0.011	0.015	0.016
0.089	0.281	0.133	0.035	0.153	0.217	0.019
0.003	0.025	0.009	0.003	0.015	0.020	0.001
0.136	0.022	0.066	0.383	0.052	0.038	0.797
0.031	0.012	0.024	0.061	0.020	0.016	0.107
0.824	0.918	0.886	0.627	0.881	0.937	0.221
0.040	0.060	0.048	0.003	0.067	0.025	0.000
0.100	0.016	0.045	–	0.039	0.026	–
0.014	0.006	0.010	–	0.007	0.009	–
0.870	0.939	0.914	–	0.925	0.949	–
0.030	0.045	0.041	–	0.036	0.025	–
0.800	0.600	0.700	0.900	0.745	0.669	0.950
0.014	0.020	0.018	0.008	0.017	0.019	0.004
0.181	0.184	0.182	0.164	0.167	0.168	0.163
–8.24	–9.30	–8.93	–7.61	–9.05	–8.92	–5.36
0.56	1.16	0.81	0.54	0.84	0.89	1.33
0.45	0.09	0.34	0.12	0.20	0.14	2.45
–4.48	–4.97	–4.87	–	–4.85	–4.87	–
0.18	0.40	0.25	–	0.20	0.38	–
0.87	0.18	0.62	–	0.39	0.25	–

tion 10 by $(n_{Ca}+n_{Sr}+n_{Mg})$ and differentiating the result with respect to the number of moles of the specific component:

$$\begin{aligned}
R\,T\ln\gamma_{Ca}^{amph} &= X_{Sr}^2 W_{CaSr} + X_{Mg}^2 W_{CaMg} + X_{Sr}X_{Mg}\left(W_{CaSr}+W_{CaMg}-W_{SrMg}\right)+X_{Sr}X_{Mg}\left(1-2X_{Ca}\right)C\\
R\,T\ln\gamma_{Sr}^{amph} &= X_{Ca}^2 W_{CaSr} + X_{Mg}^2 W_{SrMg} + X_{Ca}X_{Mg}\left(W_{CaSr}+W_{SrMg}-W_{CaMg}\right)+X_{Ca}X_{Mg}\left(1-2X_{Sr}\right)C\\
R\,T\ln\gamma_{Mg}^{amph} &= X_{Sr}^2 W_{SrMg} + X_{Ca}^2 W_{CaMg} + X_{Ca}X_{Sr}\left(W_{SrMg}+W_{CaMg}-W_{CaSr}\right)+X_{Ca}X_{Sr}\left(1-2X_{Mg}\right)C
\end{aligned} \quad (11)$$

With the assumption that the ternary interaction parameter C is zero, in conjunction with Equation 11, Equation 9 becomes:

$$\Delta\mu^{o} + 2RT\ln K_D + 2\left[W_{CaSr}^{amph}\left(X_{Ca}-X_{Sr}\right)+X_{Mg}\left(W_{SrMg}^{amph}-W_{CaMg}^{amph}\right)\right]=0 \quad (12)$$

The last term in Equation 12 will have a large effect for (Ca,Sr)-tremolites of intermediate compositions when $X_{Ca} \approx X_{Sr}$. However, because their cummingtonite contents (i.e., X_{Mg}) are very low, the last term in Equation 12 can be neglected:

$$\Delta\mu^{o} + 2RT\ln K_D + 2W_{CaSr}^{amph}\left(X_{Ca}-X_{Sr}\right)=0 \quad (13)$$

In Figure 9, -lnK_D is plotted vs. ($X_{Ca} - X_{Sr}$). If the regular solution model and the simplifications are appropriate, this plot should yield a linear relationship. The intercept is $\Delta\mu°/(2RT)$ and the slope is the binary interaction parameter W_{CaSr}^{amph}/RT. From Figure 9 it follows that the derived values of lnK_D's do indeed obey a linear relationship with respect to the M4 occupancy within the error range. Linear regression results in 59.0 ± 0.8 kJ for $\Delta\mu°$ and 9.8 ± 0.5 kJ for W_{CaSr}^{amph} (R^2 = 0.962).

For reaction 2, the equilibrium between (Ca,Sr)-diopside and fluid can be formulated in the same fashion:

$$\Delta\mu = \Delta\mu^{o} + RT\ln\frac{a_{Sr-di}^{px}\,a_{CaCl_2}^{aq}}{a_{di}^{px}\,a_{SrCl_2}^{aq}} \quad (14)$$

and

$$\Delta\mu^{o} + RT\ln K_D + W_{CaSr}^{px}\left(X_{Ca}-X_{Sr}\right)=0 \quad (15)$$

Figure 10 shows the -lnK_D vs. ($x_{Ca} - x_{Sr}$) plot for the system (Ca,Sr)-diopside/fluid. Again a linear relationship holds and values of 30.8 ± 0.5 kJ and 11.7 ± 0.6 kJ (R^2 = 0.961) were obtained for $\Delta\mu°$ and W_{CaSr}^{px}, respectively. Figure 8b shows that also the regular solution model fits the measured values well.

The interaction parameters for (Ca,Sr)-tremolite and (Ca,Sr)-diopside solid solutions are similar (W_{CaSr}^{amph} = 9.8 and W_{CaSr}^{px} = 11.7 kJ). The same is true for $\Delta\mu°$ for exchange reactions 1 and 2 if normalized to the exchange of one cation (i.e., 29.5 and 30.8 kJ).

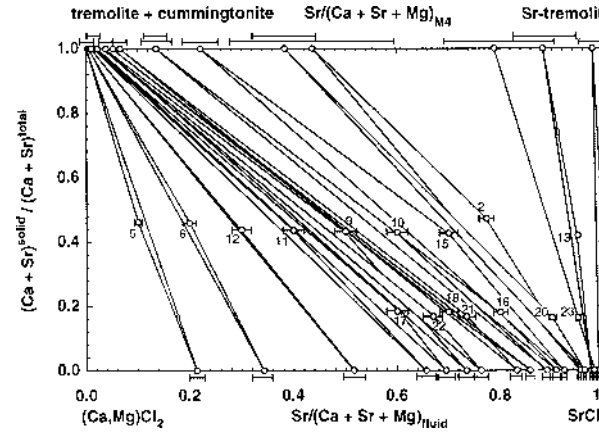

FIGURE 6. Amphibole-, fluid-, and bulk-composition plotted in the reciprocal ternary system (Ca,Sr)-tremolite–(Ca,Sr)Cl_2 as a function of X_{Sr}. Error bars denote the 2σ variations in composition. Consistent phase relations are evident by subparallel tie-lines, which are close to their respective bulk compositions. Sr fractionates strongly into the fluid.

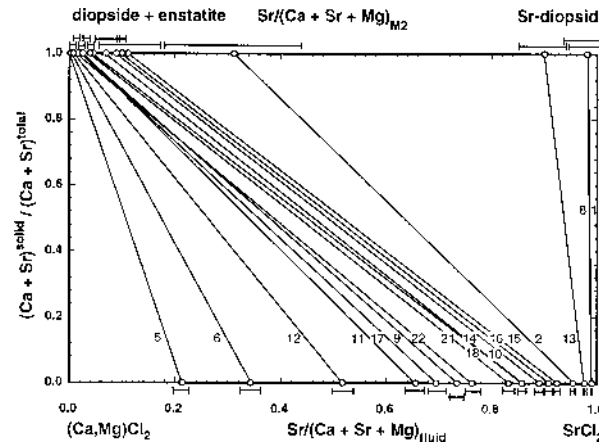

FIGURE 7. Pyroxene- and fluid-composition plotted in the reciprocal ternary system (Ca,Sr)-diopside–(Ca,Sr)Cl_2 as a function of X_{Sr}. Error bars denote the 2σ variations in composition. As in the tremolite-fluid system, Sr fractionates strongly into the fluid.

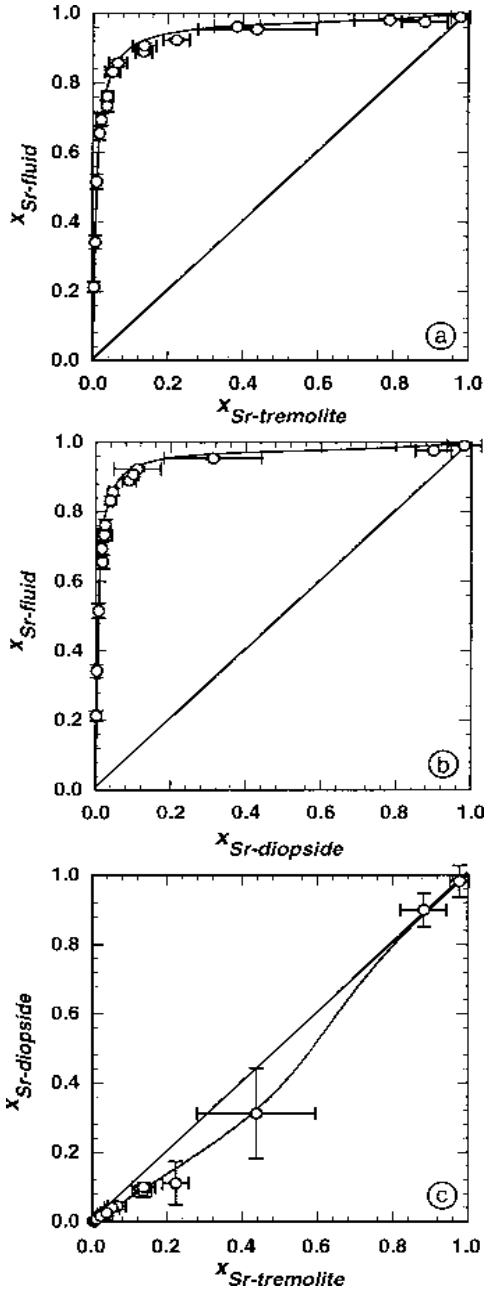

FIGURE 8. Distribution diagrams in terms of X_{Sr} between (**a**) (Ca,Sr)-tremolite and fluid, (**b**) (Ca,Sr) diopside and fluid, and (**c**) (Ca,Sr)-tremolite and (Ca, Sr)-diopside. Data are from Table 4. The curves are calculated equilibrium distributions using the derived values of $\Delta\mu^\circ = 59.0$ kJ and $W_{CaSr}^{amph} = 9.8$ kJ for (Ca,Sr)-tremolite, and $\Delta\mu^\circ = 30.8$ kJ and $W_{CaSr}^{px} = 11.7$ kJ for (Ca,Sr)-diopside.

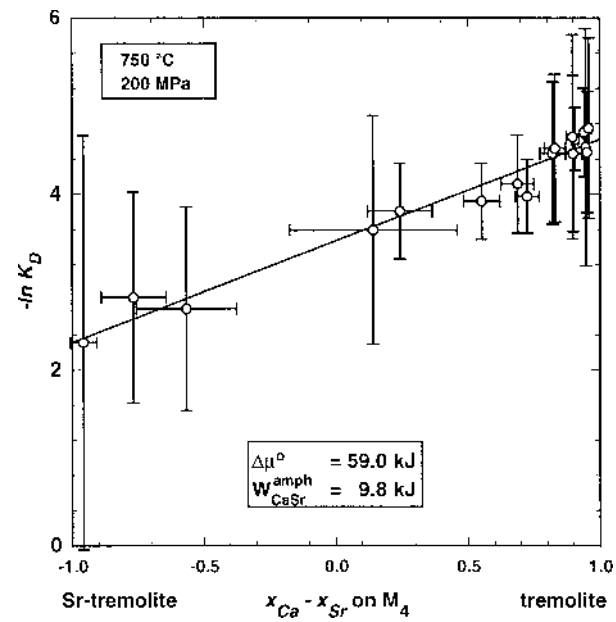

FIGURE 9. Plot of $-\ln K_D$ vs. $(X_{Ca}-X_{Sr})$ for (Ca,Sr)-tremolite. A linear relationship (regular solution model) is consistent with the experimentally derived values for K_D within errors. $\Delta\mu^\circ$ and W were calculated by linear regression.

Comparing the values of $\Delta\mu^\circ$ and W_{CaSr}, it becomes evident that $\Delta\mu^\circ$ dominates the Ca-Sr distribution between (Ca,Sr)-tremolite, (Ca,Sr)-diopside, and fluid. The excess term G_{M4}^{EM} (Eq. 10) attains its maximum for both (Ca,Sr)-tremolites and (Ca,Sr)-diopsides at $X_{Sr} \approx 0.5$ and becomes 2.5 kJ and 2.8 kJ, respectively, for the two binaries. This is less than 10% of the value of $\Delta\mu^\circ$. The difference in Gibbs free energy of Ca^{2+} and Sr^{2+} in aqueous solution is small, i.e., 5.9 kJ at 298.15 K and 0.1 MPa (Robie et al. 1979). Assuming that the two fluid species have similar heat capacities, it is mainly the difference in the Gibbs free energy of the end-members tremolite and Sr-tremolite, and diopside and Sr-diopside, i.e., their enthalpies and entropies, which governs the Ca/Sr distribution between solids and fluids and only to a minor extend the mixing behavior of Ca^{2+} and Sr^{2+} on their specific crystallographic sites.

The thermodynamic evaluation of the observed fractionation of Sr between diopside and fluid using a regular solution model for (Ca-Sr)-diopsides (see above) yields a value of 11.7 kJ for the exchange parameter W_{CaSr}^{px}. For regular solutions the critical mixing temperature, T_c, can be calculated using the relation $2RT_c = W_{CaSr}^{px}$ (e.g., Guggenheim 1967). Above T_c a continuous solid solution series exists. Under the assumption that the derived value for W_{CaSr}^{px} is independent of temperature, a critical temperature of 430 °C was calculated for the diopside–Sr-diopside solid solution series. With this value for W_{CaSr}^{px} there is no immiscibility in the (Ca,Sr)-diopside solid solution series at 200 MPa and 750 °C; W_{CaSr}^{px} must be at least 50% higher than the observed value to indicate a miscibility gap. A value of 316 °C for T_c was calculated for the tremolite-Sr-tremolite solid solution series.

PETROGENETIC IMPLICATIONS

The experimental results show that Ca^{2+} can be completely replaced by Sr^{2+} on the M4-site of amphibole and on the M2-site of clinopyroxene. For these two mineral groups, it is clear that the incorporation of Sr is governed not by structural restrictions (e.g., limited miscibility) but by the absolute elemental abundances and by the fractionation behavior within a given system.

The average abundance of Sr in upper crustal rocks is ~350 ppm with Ca/Sr ~85 (Taylor and McLennan 1985).

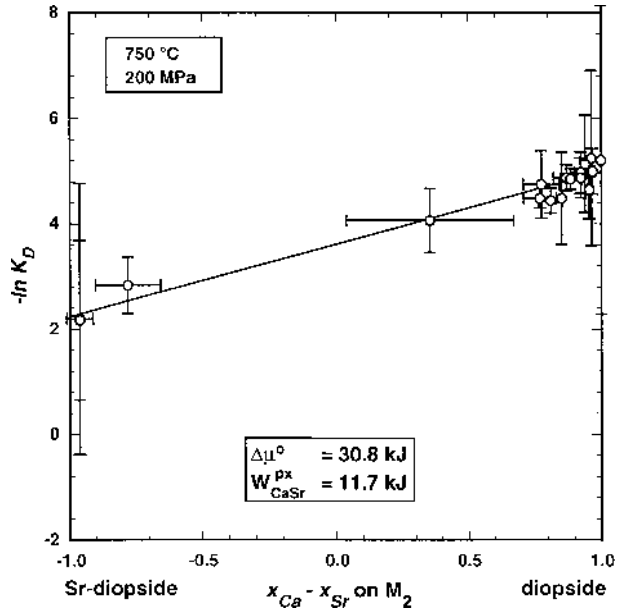

FIGURE 10. Plot of -lnK_D vs. (X_{Ca}-X_{Sr}) for (Sr,Ca)-diopside. A linear relationship (regular solution model) is consistent with the experimentally derived values for K_D within errors. $\Delta\mu^\circ$ and W were calculated by linear regression.

For the geochemical modeling of fractionation processes, partition coefficients must be available. Application of Equations 13 and 15 to such low Sr concentrations in the bulk rock [Sr/(Sr+Ca) <0.01] result in mineral/fluid partition coefficients [$D_{Sr}^{mineral/fluid} = c_{Sr}^{mineral}(wt\%) / c_{Sr}^{fluid}(wt\%)$] of 0.045 and 0.082 for coexisting (Ca,Sr)-tremolite/fluid and (Ca,Sr)-diopside/fluid pairs, respectively. The derived Sr partition coefficient for (Ca,Sr)-tremolites is almost identical to the partition coefficient of Rb in (Na,K,Rb)-richterite/fluid equilibria (Melzer, in preparation), which ranges from 0.055 and 0.064 depending on the K-concentration in richterite. In contrast, the Sr partition coefficients $D_{Sr}^{mineral/fluid}$ derived by Brenan et al. (1995), Ayers et al. (1997), and Adam et al. (1997) are considerably larger. For pargasite, augite, and chloride solution at 900 °C and 2 GPa, Brenan et al. (1995) reported a value of 1.7 for $D_{Sr}^{amph/fluid}$ and values in the range 0.48–5 for $D_{Sr}^{cpx/fluid}$. For the equilibrium of clinopyroxene and an H_2O-rich fluid at 900–1100 °C and 2–3 GPa, Ayers et al. (1997) reported $D_{Sr}^{cpx/fluid}$.values in the range 1–2. Adam et al. (1997) examined the distribution of Sr among aqueous fluid, basanitic melt, and amphibole/clinopyroxene at 1100 °C and 2 GPa. They reported $D_{Sr}^{amph/fluid}$ and $D_{Sr}^{cpx/fluid}$ values of 6.6 and 3, respectively. For amphibole/melt systems, Adam et al. (1993) give a value of 0.33–0.35 for $D_{Sr}^{amph/fluid}$ at 875–1100 °C and 1–2 GPa for pargasites and both basanitic and andesitic melt.

The partition coefficients from Brenan et al. (1995), Ayers et al. (1997), and Adam et al. (1997) were determined at higher temperatures and higher pressures, and for complex bulk compositions that are close to natural rocks. This is, however, not sufficient to explain the rather large difference in the experimental results and the reasons remain unclear. The presence of Cl^- in our fluids may play a certain role, however. Brenan et al. (1995) observed lower $D_{Sr}^{cpx/fluid}$ values for Cl-bearing fluids than for pure H_2O. On the other hand, partition coefficients for Sr between clinopyroxene and basaltic melt of 0.075 to 0.136 at 1250–1345 °C, 0.1 MPa (Ray et al. 1983) and of 0.079 at 1300 °C, 1 GPa (Skulski et al. 1994) are also much lower than the values obtained by Brenan et al. (1995), Ayers et al. (1997), and Adam et al. (1997).

It is clear that experimentally derived *partition* coefficients *D* are strictly applicable only for systems that are close to the experimental system. The essential point is that in simplified model systems, the exchange reactions are defined precisely whereas in complex natural systems they are not. The *distribution* coefficients K_D and the equilibrium constants as derived here are thermodynamically more meaningful values and more universal; an understanding or at least reasonable assumptions of the mixing behavior of the phases involved is required, however. Comparing partition coefficients derived in different systems is a rather dangerous task.

Natural examples, such as the metaeclogite of Bjørkedalen, SW Norway, with whole-rock concentrations of up to 2.4 wt% SrO (Brastad 1985) are, however, well-suited for comparison of derived distribution coefficients with those predicted from studies of exchange reactions. This rock was metasomatized by an anomalously Sr-rich fluid. The maximum contents of Sr-bearing components are up to 27 mol% $Sr_2Al_2Si_2O_8$ in plagioclase, 20 mol% $Sr_2Al_3Si_3O_{12}(OH)$ in epidote, 51 mol% $Na_4Sr_8[Al_{20}Si_{20}O_{80}]\cdot 24H_2O$ in thomsonite, 2 mol% $Sr_5(PO_4)_3(OH)$ in apatite, and 1 mol% $Sr_2Mg_5Si_8O_{22}(OH)_2$ in amphibole. The experimentally determined distribution coefficient K_D is used to derive the Ca/Sr-ratio of the fluid that caused the metasomatism. Using a value for K_D of 1.2×10^{-4} for Sr-poor tremolites (Fig. 9) a Ca/Sr ratio (wt%) of 0.55 was calculated for the coexisting fluid using Equation 16:

$$\left(c_{Ca}^{fluid} / c_{Sr}^{fluid}\right)^2 = K_{D(Sr-Ca)}^{amph-fluid} \bullet (c_{Ca}^{amph} / c_{Sr}^{amph}) \quad (16)$$

Experimentally determined equilibria between (Ca,Sr)-anorthite and fluid are available from Lagache and Dujon (1987) at 750 °C and 200 MPa, and from Kotelnikov et al. (1989) at 700–800 °C and 100–200 MPa. Application of these results to the plagioclase in the Bjørkedalen metaeclogite leads to a Ca/Sr ratio (wt%) in the fluid of 0.81 for the distributions derived by Lagache and Dujon (1987), and of 0.79 using the results from Kotelnikov et al. (1989). Considering that neither the amphibole nor the plagioclase in the Bjørkedalen metaeclogite are pure (Ca,Sr)-solid solutions, the derived Ca/Sr ratios (wt%) are in good agreement with the value of 0.55 derived here.

ACKNOWLEDGMENTS

This work has been supported by the German Science Foundation (grants He2015/1-4 and Fr 557/7) as part of the program "Experimental studies on element distributions between minerals, melts and fluids in geological relevant systems." We thank F. Galbert (ZELMI, TU Berlin) and D. Rhede (GeoForschungsZentrum Potsdam) for their kind help with the EMP and R. Nähter (TU Berlin) with the AAS. The thoughtful and detailed reviews by J.C. Ayers and J.M. Brenan are gratefully acknowledged.

REFERENCES CITED

Adam, J., Green, T.H., Sie, S.H., and Ryan, C.G. (1997) Trace element partitioning between aqueous fluids, silicate melts and minerals. European Journal of Mineralogy, 9, 569–584.

Ayers, J.C., Dittmer, S.K., and Layne, G.D. (1997) Partitioning of elements between peridotite and H_2O at 2.0–3.0 GPa and 900–1100 °C. and application to models of subduction zone processes. Earth and Planetary Science Letters, 150, 381–398.

Ayers, J.C. and Watson, E.B. (1993) Apatite/ fluid partitioning of rare-earth elements and strontium; experimental results at 1.0 GPa and 1000 degrees C and application to models of fluid-rock interaction. Chemical Geology, 110, 299–314.

Benna, P. (1982) Ca-Sr substitution in clinopyroxenes along the join $CaMgSi_2O_6$-$SrMgSi_2O_6$. Tschermaks Mineralogische und Petrographische Mitteilungen, 30, 37–46.

Benna, P., Chiari, G., and Bruno, E. (1987) Structural modification in clinopyroxene solid solutions: the Ca-Mg and Ca-Sr substitutions in diopsid structure. Mineralogy and Petrology, 36, 71–84.

Brastad, K. (1985) Sr metasomatism, and partition of Sr between the mineral phases of a meta-eclogite from Bjorkedalen, West Norway. Tschermaks Mineralogische und Petrographische Mitteilungen, 34, 87–103.

Brenan, J.M., Shaw, H.F., Ryerson, F.J., and Phinney, D.L. (1995) Mineral-aqueous fluid partitioning of trace elements at 900 degrees C and 2.0 GPa; constraints on the trace element chemistry of mantle and deep crustal fluids. Geochimica et Cosmochimica Acta, 59, 3331–3350.

Brenan, J.M. and Watson, E.B. (1991) Partitioning of trace elements between olivine and aqueous fluids at high P-T conditions; implications for the effect of fluid composition on trace-element transport. Earth and Planetary Science Letters, 107, 672–688.

Della Ventura, G. and Robert, J.-L. (1990) Synthesis, XRD and FTIR studies of strontium richterites. European Journal of Mineralogy, 2, 171–175.

Gottschalk, M., Najorka, J., and Andrut, M. (1998) Structural and compositional characterization of synthetic (Ca,Sr)-tremolites and (Ca,Sr)-diopsides. Physics and Chemistry of Minerals, in press.

Grapes, R. and Watanabe, T. (1984) Al-Fe^{3+} and Ca-Sr^{2+} epidotes in metagreywacke-quartzofeldspathic schist, Southern Alps, New Zealand. American Mineralogist, 69, 490–498.

Guggenheim, E.A. (1967) Thermodynamics: an advanced treatment for chemists and Ohysicists. Elsevier Science Publishers.

Kotelnikov, A.R. and Chernysheva, I.V. (1995) Excess free energies of mixing of Sr, Ba-bearing binary feldspar solid solutions (experimental data). Mineralogical Magazine, 59, 79–91.

Kotelnikov, A.R., Chernysheva, I.V., Romanenko, I.M., and Tikhomirova, E.I. (1989) Experimental determination of energy of mixing of Ca-Sr-anorthites from data on cation-exchange equilibria. Geochimia, 11, 1575–1586.

Kroll, H., Kotelnikov, A.R., Göttlicher, J., and Valyashko, E.V. (1995) (K,Sr)-feldspar solid solutions: the volume behaviour of heterovalent feldspars. European Journal of Mineralogy, 7, 489–499.

Lagache, M. and Dujon, S.C. (1987) Distribution of strontium between plagioclases and 1 molar aqueous chloride solutions at 600 degrees C, 1.5 kbar and 750 °C, 2 kbar. Bulletin de Mineralogie, 110, 551–561.

Ray, G.L., Shimizu, N., and Hart, S.R. (1983) An ion microprobe study of partitioning of trace elements between clinopyroxene and liquid in the system diopside-albite-anorthite. Geochimica et Cosmochimica Acta, 47, 2131–2140.

Robert, J.L., Della Ventura, G., Raudsepp, M., and Hawthrone, F.C. (1993) Rietveld structure refinement of synthetic strontium-rich potassium-richterites. European Journal of Mineralogy, 5, 199–213.

Robie, R.A., Hemingway, B.S., and Fisher, J.R. (1979) Thermodynamic properties of minerals and related substances at 298.15 K and 1 bar (10^5 pascals) pressure and at higher temperatures. U.S. Geological Survey Bulletin, 1452, 456.

Shannon, R.D. (1976) Revised effective ionic radii and systematic studies of interatomic distances in halides and chalcogenides. Acta Crystallographica Section A, 32, 751–767.

Skulski, T., Minarik, W., and Watson, E.B. (1994) High-pressure experimental trace-element partitioning between clinopyroxene and basaltic melts. Chemical Geology, 117, 127–147.

Taylor, S.R. and McLennan, S.M. (1985) The Continental Crust: Its Composition and Evolution, 312 p. Blackwell Scientific, London.

Theye, T. and Seidel, E. (1988) Fluorine, lithium and strontium metasomatism in high pressure metamorphic rocks, Crete. Fortschritte der Mineralogie, Beiheft 66, 157.

Wohl, K. (1946) Thermodynamic evaluation of binary and ternary liquid systems. Transactions of the American Institute of Chemical Engineering, 42, 215–249.

Zimmermann, R., Gottschalk, M., Heinrich, W., and Franz, G. (1997a) Experimental Na-K distribution between amphiboles and aqueous chloride solutions, and a mixing model along the richterite –K-richterite join. Contributions to Mineralogy and Petrology, 126, 252–264.

Zimmermann, R., Knop, E., Heinrich, W., Pehlke, I., and Franz, G. (1997b) Disequilibrium in cation exchange experiments between Na-richterite – K-richterite and aqueous solutions: effects of fractional crystallization. European Journal of Mineralogy, 9, 97–114.

MANUSCRIPT RECEIVED JANUARY 22, 1998
MANUSCRIPT ACCEPTED OCTOBER 22, 1998
PAPER HANDLED BY GRAY E. BEBOUT